Calcif Tissue Int (2015) 96:80–87
DOI 10.1007/s00223-014-9934-8

ORIGINAL RESEARCH

Thyroid Hormone Attenuates Vascular Calcification Induced by Vitamin D3 Plus Nicotine in Rats

Jing Zhang · Jin-Rui Chang · Xiao-Hui Duan · Yan-Rong Yu · Bao-Hong Zhang

Received: 8 May 2014 / Accepted: 17 November 2014 / Published online: 23 November 2014

Abstract Thyroid hormones (THs) including thyroxine (T_4) and triiodothyronine (T_3) play critical roles in bone remodeling. However, the role and mechanism of THs in vascular calcification (VC) have been unclear. To explore the pathophysiological roles of T3 on VC, we investigated the changes in plasma and aortas of THs concentrations and the effect of T3 on rat VC induced by vitamin D3 plus nicotine (VDN). VDN-treated rat showed decreased plasma T3 content, increased vascular calcium deposition, and alkaline phosphatase (ALP) activity. Administration of T3 (0.2 mg/kg body weight IP) for 10 days greatly reduced vascular calcium deposition and ALP activity in calcified rat aortas when compared with controls. Concurrently, the loss of smooth muscle lineage markers α-actin and SM22a was restored, and the increased bone-associated molecules, such as runt-related transcription factor2 (Runx2), Osterix, and osteopontin (OPN) levels in calcified aorta, were reduced by administration of T3. The suppression of klotho in calcified rat aorta was restored by T3. Methimazole (400 mg/L) blocked the beneficial effect of T3 on VC. These results suggested that T3 can inhibit VC development.

J. Zhang (✉)
School of P.E. and Sports Science, Beijing Normal University, Beijing 100875, China
e-mail: zhangjing@bnu.edu.cn

J.-R. Chang · X.-H. Duan · Y.-R. Yu
Laboratory of Cardiovascular Bioactive Molecules, School of Basic Medical Sciences, Peking University, Beijing 100191, China

B.-H. Zhang (✉)
Hospital of Tsinghua University, Beijing 100084, China
e-mail: hongbaozhang@163.com

Keywords Thyroid hormone · Vascular calcification · Vitamin D_3 plus nicotine

Introduction

Thyroid hormones (THs) are synthesized by the thyroid gland, including thyroxine (T_4) and triiodothyronine (T_3). T_4 is the major secreted hormone, yet, T_3 is classically considered as the active and more potent hormone since it binds to thyroid hormone receptors (TRs) with higher affinity than T_4 [1].The clinical effects of THs on bone have been interested for more than a century. THs are required for skeletal development and establishment of peak bone mass [2, 3]. In adults, T3 regulates bone turnover and bone mineral density [4], and normal euthyroid status is essential to maintain optimal bone strength [5, 6]. In addition, alterations in THs levels have a profound effect on the cardiovascular system [7], which includes changes in myocardial contractility, heart rate, and resistance of peripheral vasculature [8–10]. Recently, mRNAs for TR isoforms were identified in aortic and coronary smooth muscle cells [11], suggesting that THs may play a direct role in vascular smooth muscle. Tatar et al. reported that serum-free T3 levels were inversely associated with arterial stiffness in hemodialysis patients without diabetes [12]. These findings hinted that THs could involve in calcium homeostasis regulating and correlate with vascular calcification (VC).

VC is a well-recognized pathological entity associated with cardiovascular morbidity and mortality [13]. Recent studies have shown that VC is an active, cell-regulated process, with many similarities to bone formation [14, 15]. Vascular smooth muscle cell (VSMC) can lose the expression of smooth muscle lineage markers and begin to

express osteogenic markers and deposit a mineralized bone-like matrix [14–19]. During the mineralization of VSMC, runt-related transcription factor2 (Runx2), a transcription factor expressed at early stages of osteoblast differentiation, is upregulation [20], and in concert with osterix by regulating the expression of osteoblast-related gene [21], such as osteopontin (OPN) contributes to VC [22]. Recent study suggested that klotho knockdown can accelerate VSMC calcification through a Runx2-dependent pathway. Klotho, a cofactor for fibroblast growth factor 23 (FGF-23) signaling, is locally expressed in VSMC, and protects against VC by mediating FGF23 inhibitory effects on matrix mineralization [23]. However, the direct target genes of THs in VSMCs are poorly understood.

In our work, we investigated the change of THs concentration in plasma and the effect of T3 on phenotype transition in vitamin D3 plus nicotine-(VDN) induced VC rats. We observed the effect of T3 on Runx2, Osterix, OPN and klotho expression, and lineage markers of VSMC to investigate the mechanisms of T3 on VC.

Materials and Methods

Materials

Male Sprague–Dawley (SD) rats (200 ± 10 g) were purchased from the Animal Center, Peking University Health Sciences Center. All animal care and experimental protocols complied with the Animal Management Rule of the Ministry of Health, People's Republic of China (Document No. 55, 2001). Rats were housed under standard conditions (room temperature 20 ± 8 °C, humidity 60 ± 10 %, lights from 6:00 to 18:00). T3 was from Merck (Darmstadt, German). Methimazole (MMI) and Vitamin D3 were from Sigma (St Louis, MO, USA). The calcium assay kit was from Zhongsheng Biosino Bio-technology and Science (Beijing, China). The alkaline phosphatase (ALP) activity kit was from Beihuakangtai Clinical Reagent Co., (Beijing, China). Radioimmunoassay kits for rat serum T3 and T4 were provided by Beijing Free Biological Technology (Beijing, China). Anti-SM22α antibody was from abcam (Cambridge, UK). Antibodies against α-actin, β-actin, klotho, and OPN antibody were from Santa Cruz Biotechnology (Santa Cruz, CA, USA). Nitrocellulose membrane was from Hybond-C (Amersham Life Science, England), and an enhanced chemiluminescence kit was from Beijing Applygen Technologies (Beijing, China). Trizol was from GIBCOL (BRL, Rockville, MD), and dNTP, M-MuLV RT, Oligo (dT) 15 primer, and Taq DNA polymerase were from Promega (Madison, WI). Oligonucleotides were synthesized by Sai Baisheng Biotechnology (Beijing, China). All other chemicals and reagents were of analytical grade.

Animal Model

Male SD rats were randomly assigned to 5 groups ($n = 8$ in each group).VC was induced by VDN as described previously [24]. In brief, the rats were injected with vitamin D_3 (300,000 IU/kg) intramuscularly and given nicotine intragastrically with peanut oil (5 ml/kg, 5 mg nicotine dissolved in 1 ml peanut oil) at 8 am, and nicotine in peanut oil was administered again at 8 pm on the same day. Rats in control group received normal saline intramuscularly and two gavages of peanut oil without nicotine (5 ml/kg) instead. The rats in Cal+T3 group were the VDN rats daily injection of T3 (0.2 mg/kg body weight IP) for 10 days. MMI (400 mg/L) was added to the drinking water for 4 weeks for VDN alone or plus T3 injection. After 4 weeks, all rats fasted overnight but had free access to water.

At the end of the experiment, hemodynamic variables were measured with use of PowerLab of BL-420F instruments (TaiMeng Ltd., Chengdu, China). After hemodynamic parameters were measured, a blood sample was drawn and mixed with 1 mg/ml EDTA-Na_2 and 500 KIU/ml aprotinin. Plasma was obtained by centrifugation at $3{,}000 \times g$ for 15 min at 4 °C and stored at −70 °C. The intact aorta was then stored at −70 °C.

Detection of VC

The calcium content was measured by use of an atomic absorption spectrophotometer (novAA 300, Analytik Jena AG, Germany) at 422.7 nm as we described. Calcium content of the aorta was normalized to tissue dry weight. The ALP activity in aortic tissue was measured with the use of an ALP assay kit and results were normalized to the total protein concentration.

Radioimmunoassay of Free T3 and Free T4 Levels

The plasma samples were prepared and pre-treated with aprotinin (500 KIU/ml). Plasma was loaded onto a Sep-Pak ^{18}C cartridge after equilibration with normal saline. The cartridge was washed with 2.5 ml normal saline and 10 % acetonitrile in 0.1 % trifluoroacetic acid, and then eluted with 2 ml of 50 % acetonitrile in 0.1 % trifluoroacetic acid. The elution was lyophilized and subjected to radioimmunoassay. The range of the standard curve of T3 was 0.50–8.0 ng/ml, in which a double-logarithmic scale showed a linear relationship with $r^2 = 0.999$. All samples were within the range of the standard curve. The detection limit was calculated to be 0.25 ng/ml. The intra- and

interassay coefficients of variation were validated within our work and were 10 and 15 %, respectively. There is no cross-reactivity found with rat T4. The range of the standard curve of T4 was 20–320 ng/ml, in which a double-logarithmic scale showed a linear relationship with $r^2 = 0.999$. All samples were within the range of the standard curve. The detection limit was calculated to be 3.0 ng/ml. The intra- and interassay coefficients of variation were validated within our work and were 10 and 15 %, respectively. There is no cross-reactivity found with rat T3.

Real-Time PCR Analysis

Total RNA from aorta tissues was isolated and reverse transcribed by use of a reverse-transcription system (Promega, Madison, WI, USA). In total, 20 μL of the reaction mixture underwent real-time PCR, and then evaluated by use of SYBR Green I fluorescence. The rat primers were for Runx2 (149 bp), forward, 5′-AGT GAT TTA GGG CGC ATT CC-3′ and reverse, 5′-GGT GGG GAG GAT TGT GTC TG-3′; Osterix (148 bp), forward, 5′-TTG GTT AGG TGG TGG GCA GG-3′ and reverse, 3′-GAG GTG GGG TGC TGG ATA GG-5′; and β-actin (207 bp), forward, 5′-CAC CCG CGA GTA CAA CCT TC-3′ and reverse, 5′-CCC ATA CCC ACC ATC ACA CC-3′ as a normalization control. All amplification reactions involved use of the Mx3000 Multiplex Quantitative PCR System (Stratagene, La Jolla, CA, USA). After being denatured at 95 °C for 7 min, the solution underwent PCR for Runx2 at 95 °C for 30 s, 60 °C for 30 s, and 72 °C for 40 s for 40 cycles and for Osterix at 95 °C for 30 s, 60 °C for 30 s, and 72 °C for 40 s for 40 cycles.

Western Blot Analysis

Protein extracts from aortas were resuspended in sample buffer that contained 2 % SDS, 2 % mercaptoethanol, 50 mmol/L Tris–HCl (pH 6.8), 10 % glycerol, and 0.05 % bromophenol blue. The protein mixture was then placed in boiling water for 10 min and briefly centrifuged at a low speed. The denatured protein samples were resolved on a 10 % SDS–polyacrylamide gel in running buffer containing 25 mmol/L Tris, 192 mmol/L glycine, and 0.1 % SDS. The proteins were then transferred to a nitrocellulose membrane for 3 h at 4 °C at 200 mA in a transfer buffer containing 25 mmol/L Tris, 192 mmol/L glycine, and 20 % methanol. Non-specific protein binding was blocked by incubating the membrane with 5 % non-fat dry milk in TBS-T (20 mmol/L Tris–HCl (pH 7.6), 150 mmol/L NaCl, and 0.02 % Tween 20) for 1 h at room temperature with agitation. A goat anti-rat OPN primary antibody (1:500), anti-klotho (1:200), anti-SM22α (1:1,000), or anti-α-actin (1:2,000) were added to the membrane in TBS-T and incubated at 4 °C overnight with agitation. The secondary antibody was diluted in TBS-T (1:2,000 dilution) and applied to the membrane, and the reaction was incubated at room temperature for 1 h with agitation and underwent enhanced chemiluminescence detection. Between each of the steps, the membrane was washed 3 times for 10 min each with TBS-T at room temperature. Protein expression was analyzed by NIH image software and normalized to β-actin expression.

Statistical Analysis

All statistical analyses were carried out using the Graphpad Prism 5.0 software. Data are expressed as mean ± SEM. Student's *t* test was used to compare results between 2 groups. One-way ANOVA, followed by a Student–Newman–Keuls test, was used to compare results between more than 2 groups. $p < 0.05$ was considered statistically significant.

Results

Plasma T3 and T4 was Decreased in Rats with VC

Compared with the control group, VDN rats showed significantly decreased immunoreactive-T3 (ir-T3) and ir-T4 content in plasma by 25 and 12 %, respectively, (both $p < 0.05$) (Fig. 1).

T3 Treatment Improved Hemodynamic Function and Attenuated VC

In the rat model of VC, heart weight (HW)/body weight (BW), SBP, LVSP, and +LV d*p*/d*t* max were significantly elevated, by 11.6, 14.6, 23.0, and 113.5 %, respectively (all $p < 0.05$), as compared with controls (Table 1). Compared with VC alone, T3 treatment reduced HW/BW, SBP, and +LV d*p*/d*t* max by 11.4 %, 10.4, and 27.6 % ($p < 0.05$) (Table 1).

In VDN rats, aortic ALP activity and calcium level were significantly increased by 223.4 and 318.8 % (both $p < 0.01$), respectively, as compared with controls. Compared with VC alone, T3 treatment decreased aortic ALP activity and calcium content by 65.2 and 68.3 %, respectively (both $p < 0.01$) (Fig. 2). MMI, the most potent antithyroid drug, treatment abolished the protective effects of T3 on VC in VDN rats. MMI treated alone did not affect the aortic ALP activity and calcium content in VDN rats.

T3 Decreased the Aortic mRNA Level of Runx2 and Osterix and Protein Level of OPN and Increased Protein Level of klotho

Runx2, Osterix mRNA levels, and OPN protein level were higher by 180, 43.9, and 257 %, and klotho protein level

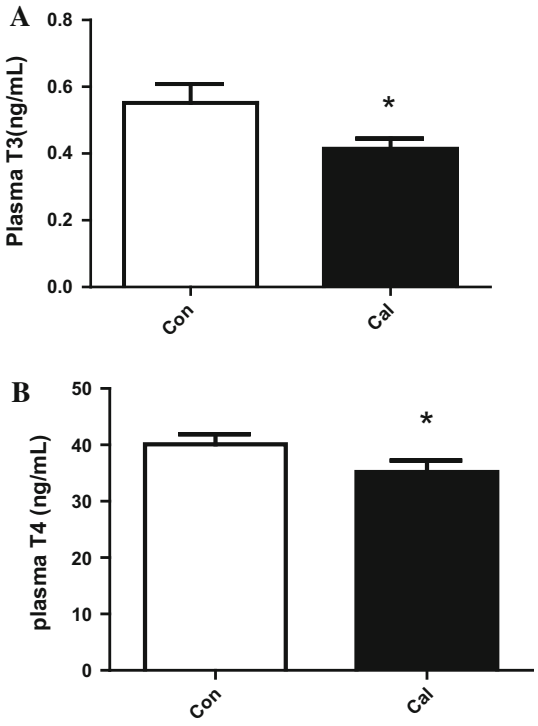

Fig. 1 Changes of triiodothyronine (T_3) (**a**) and thyroxine (T_4) (**b**) plasma concentrations in rat with vascular calcification (VC). *Ctrl* control, *Cal* calcification. Data are shown as mean ± SEM, $n = 6$ at least in each group. *$p < 0.05$ versus Con

was lower by 53 % in VDN rats aortic tissue than in control rats. T3 treatment prevented the enhanced expression of Runx2, Osterix mRNA, and OPN protein by 45.2, 38.6, and 25.2 %, respectively (all $p < 0.01$) (Figs. 3, 4), and increased the klotho protein level by 92 % ($p < 0.01$) compared with that in rat aortas with VC alone. MMI treatment withdrew the effect of T3 on VDN rats. There is no significant change between VDN rats and MMI-treated VDN rats.

T3 Retarded Loss of Lineage Markers in VSMCs

Because the phenotype transition of VSMCs is associated with VC in vitro and in vivo, we further investigated the protein expression of smooth muscle lineage markers. Compared with normal vessels, VDN vessels showed decreased protein level of α-actin and SM-22α by 76.4 and 63.5 % (both $p < 0.01$), respectively (Fig. 5). T3 treatment prevented the reduction in α-actin and SM-22α by 409 and 130 % (both $p < 0.01$), respectively (Fig. 5). MMI cancels the effects of T3 in VDN VSMCs. There is no significant change between VDN rats and MMI-treated VDN rats.

Discussion

In the present study, we found that administration of vitamin D3 and nicotine to rats resulted in serious VC, with systolic hypertension and left ventricular concentric hypertrophy, which suggests the reduced arterial compliance and the compensatory potentiation of cardiac contractile function. T3 treatment attenuated calcification and prevented the loss of lineage markers in rat aortas. Furthermore, T3 restored klotho expression and downregulated Runx2, Osterix, and OPN expression in calcified aortas. MMI is known to interfere with the synthesis and release of THs. MMI treatment significantly decreased plasma T3 content in VDN rats and abolished the effects of T3 on VC in VDN rats. These results suggested that T3 could be a key endogenous protective factor in VC.

Table 1 Blood pressure, cardiac function, body weight, and left ventricle ratio of rats

	Con	Cal	Cal + T3	Cal + MMI	Cal + T3 + MMI
HW/BW(mg/g)	2.84 ± 0.18	3.17 ± 0.42*	2.81 ± 0.12#	2.43 ± 0.12#&	2.49 ± 0.19&
HR (beats/min)	336.3 ± 40.6	398.2 ± 27.45*	370.5 ± 37.6	267.9 ± 24.7##&&	310.6 ± 53.65&
SBP (mmHg)	95.8 ± 8.9	109.8 ± 7.3*	98.4 ± 3.6#	91.1 ± 3.6#	98.4 ± 9.0#
MBP (mmHg)	80.9 ± 3.2	94.1 ± 6.1*	70.1 ± 8.9##	71.9 ± 11.5##	83.4 ± 9.7
Pluse pressure (mmHg)	27.5 ± 4.9	47.5 ± 8.9*	40.6 ± 11.3	23.3 ± 3.0#&	23.4 ± 3.8#
LVSP(mmHg)	97.4 ± 9.5	119.8 ± 10.3*	114.0 ± 6.4	94.5 ± 8.3#&	101.9 ± 16.5
LVEDP (mmHg)	−8.18 ± 1.26	−4.89 ± 1.20**	−5.95 ± 2.00	−5.10 ± 0.44	−5.19 ± 1.90
+LVdp/dtmax (mmHg/s)	2,594 ± 800	5,539 ± 2,190*	5,071 ± 1,669*	3,800 ± 1,053	4,012 ± 771
−LVdp/dtmax (mmHg/s)	−2,354 ± 859	−2,744 ± 363	−3,248 ± 478	−3,307 ± 388	−3,149 ± 800

Values are mean ± SEM, $n = 6$ in each group

HW heart weight, *BW* body weight, *HR* heart rate, *SBP* systolic blood pressure, *DBP* diastolic blood pressure, *LVSP* left ventricular systolic pressure, *LVEDP* left ventricular end diastolic pressure, ± *LV* dp/dtmax left ventricular peak rate of contraction and peak rate of relaxation were measured in vivo, *T3* triiodothyronine, *MMI* methimazole. *Con* control, *Cal* calcification

* $p < 0.05$, ** $p < 0.01$ versus control, # $p < 0.05$, ## $p < 0.01$ versus Cal, & $p < 0.05$, && $p<0.01$ versus Cal + T3, respectively

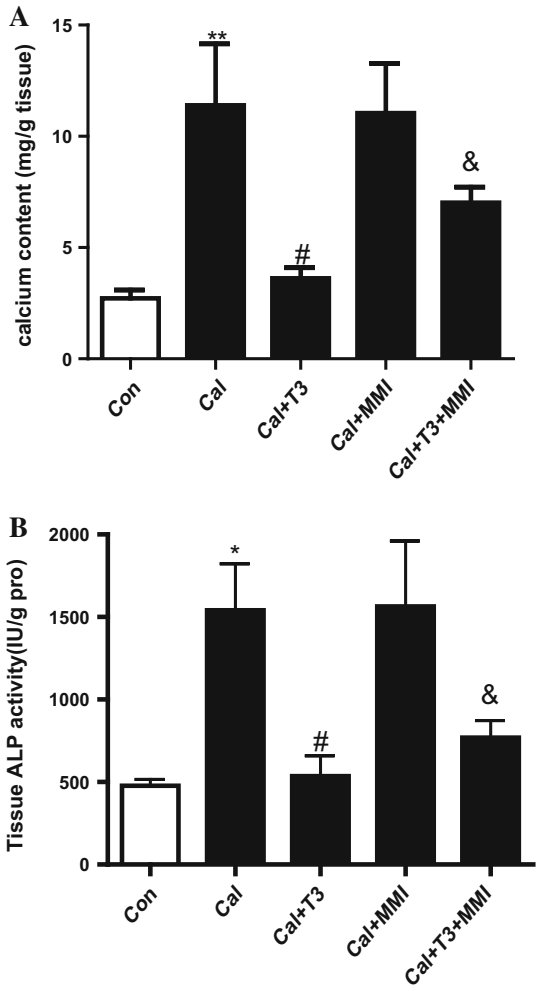

Fig. 2 Triiodothyronine (T_3) treatment decreased aortic calcium content (**a**) and alkaline phosphatase (ALP) activity (**b**) in vitamin D_3 plus nicotine (VDN) rats. *Ctrl* control, *Cal* calcification, *MMI* methimazole. Data are expressed as mean ± SEM, $n = 6$ at least in each group. $^{*}p < 0.05$, $^{**}p < 0.01$ versus Con, $^{\#}p < 0.05$ versus Cal; & $p < 0.05$ versus Cal + T3

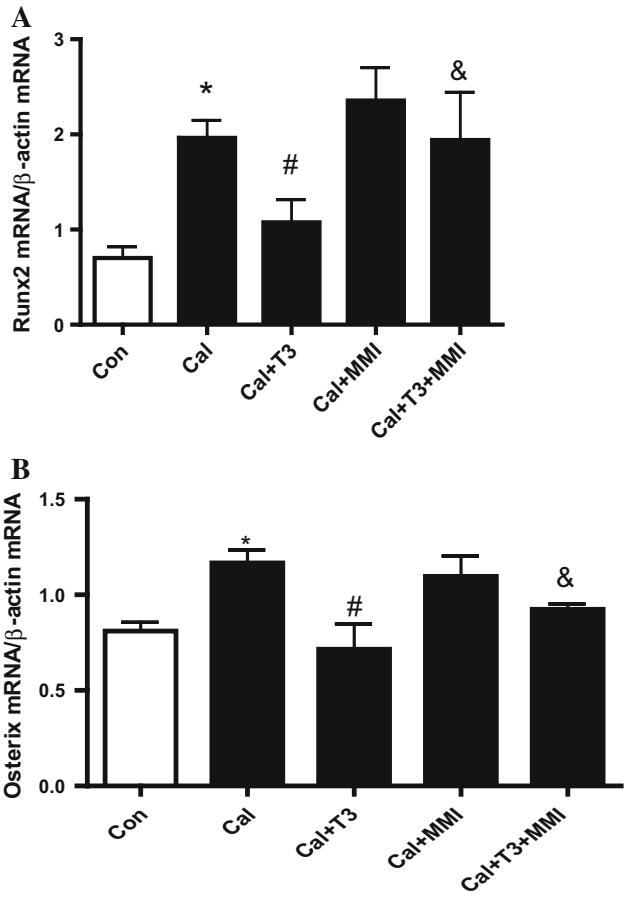

Fig. 3 Triiodothyronine (T_3) treatment decreased the aortic mRNA level of Osterix and runt-related transcription factor2 (Runx2). Quantitative real-time PCR of mRNA levels of **a** Osterix and **b** Runx2 in rat aortas. Data are expressed as mean ± SEM, $n = 4$. $^{*}p < 0.05$ versus Con, $^{\#}p < 0.05$ versus Cal; & $p < 0.05$ versus Cal + T3

Lots of clinical studies showed that ectopic calcification in blood vessels is often accompanied by either decreased bone mineral density or disturbed bone turnover. This contradictory association has been observed in the general population [25], in osteoporosis and chronic kidney disease patients [26, 27]. The term calcification paradox has been coined to refer to this counterintuitive observation [28]. It is urgent to find an endogenous factor, which not only can be used to treat osteoporosis, but also have an inhibiting effect on VC. The profound effects of THs on bone mineralization have been confirmed in clinical and pharmacological studies. Recently study showed that serum-free T3 levels were inversely associated with arterial stiffness in hemodialysis patients [12]. Analysis performed among health subjects showed that free T4 level was inversely associated with coronary artery calcification [29] and independently associated with carotid intima-media thickness [30] in euthyroid subjects. Sato et al. reported that aortic smooth muscle tissues from methimazole-induced hypothyroid rats showed increasing calcium content compared with that from the control euthyroid animals, whereas T3 treatment reduced calcium content [31]. These results indicated that normal THs level involved in the prevention of VC; however, the alteration of endogenous T3 content and the effect of T3 in VC were still unclear. In the present study, plasma T3 levels were significantly decreased in VDN-induced rat VC. T3 treatment attenuated the calcium content and ALP activity in rat aortas with VC, improved the hemodynamic function. MMI blocked the therapeutic effect of T3 on VC. These results indicated that T3 could be an endogenous anti-VC factor and might be a novel target in keeping calcium homeostasis. However, the

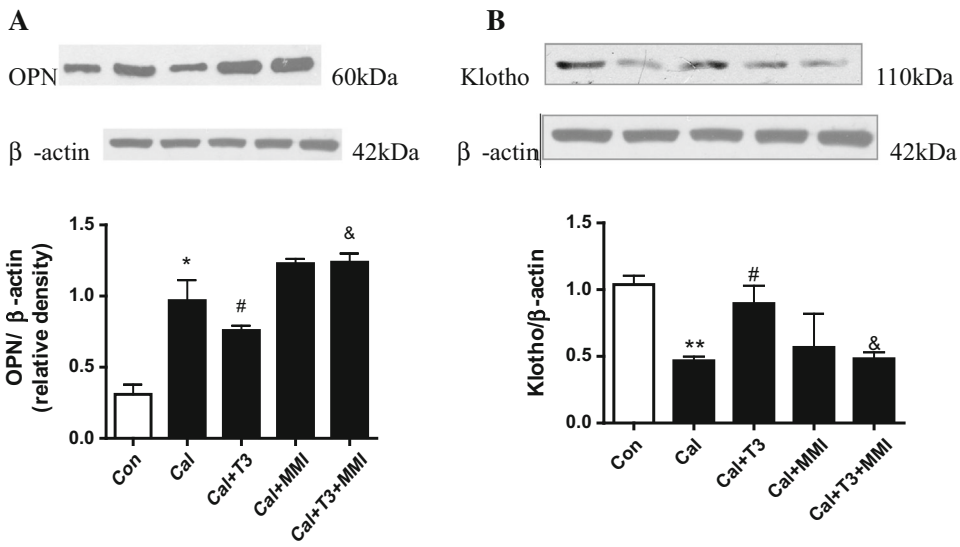

Fig. 4 Triiodothyronine (T_3) treatment decreased protein level of osteopontin (OPN) and increased protein level of klotho. Western blot analysis of protein level of **a** osteogenic marker OPN and **b** klotho in rat aortas. β-actin was a loading control. Data are expressed as mean ± SEM, $n = 4$. $^{*}p < 0.05$, $^{**}p < 0.01$ versus Con; $^{\#}p < 0.05$ versus Cal; & $p < 0.05$ versus Cal + T3

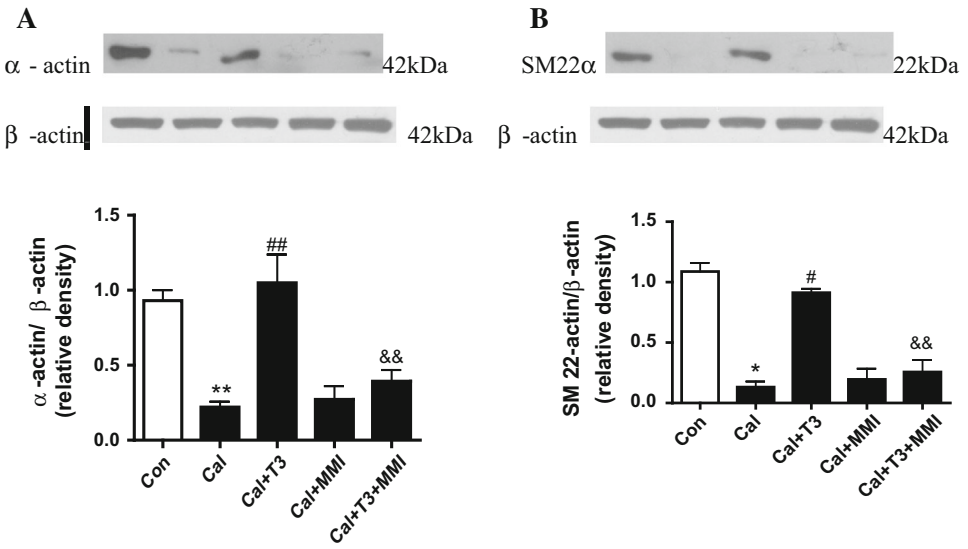

Fig. 5 Triiodothyronine (T_3) treatment retarded smooth muscle cell phenotypic transition in rat aortas with vascular calcification. Western blot analysis of protein level of **a** α- actin and **b** lineage marker α-smooth muscle actin (α-SMA) in rat aortas. Data are expressed as mean ± SEM, $n = 4$. $^{*}p < 0.05$, $^{**}p < 0.01$ versus Con, $^{\#}p < 0.05$, $^{\#\#}p < 0.01$ versus Cal, && $p < 0.01$ versus Cal + T3

physiological and direct target genes of T3 in VSMCs are not known.

VC is an active and complex process, with VSMC phenotype transformation. Once the osteogenic phenotype is induced, cells of the vascular wall begin to express osteogenic markers [14–19]. An increasing number of studies have implicated the upregulation of Runx2 expression in the osteogenic differentiation of VSMCs [32–34].The transcription factor Runx2 is one of the three mammalian members of the Runt-related transcription family [35]. Runx2 has originally been identified as an essential transcription factor in osteoblast differentiation, bone matrix gene expression, and consequently bone mineralization [20]. Runx2 and osterix, which is activated downstream of Runx2 [21, 36], regulate the expressions of various bone marker genes, including ALP, osteocalcin (OCN), OPN and finally, mineralization of bone nodules [37]. Recent study showed that suppression of klotho was associated with upregulation of Runx2 and induced VSMC phenotype transformation [23]. Klotho, known as α-Klotho, a 130-kDa single-pass transmembrane protein, expresses at high levels in renal distal tubular epithelial cells, and to a lesser extent in VSMC. Vascular-produced Klotho acted as an endogenous inhibitor of calcification and as a cofactor for FGF-23 signaling, and mediated vascular resistance to FGF23 in VC [24]. We showed that T3 treatment restored the expression of klotho and decreased the expression of Runx2, Osterix, and OPN, prevented the loss of the lineage markers, SM22α and α-actin. Furthermore, MMI completely abolished the effect of T3 on kotho, Runx2, Osterix, and OPN expression, which demonstrated that the effect was mediated by T3. Therefore, T3 attenuated VC in part by balancing stimulation and

inhibition of VSMC calcification, thus maintaining phenotype stabilization.

In conclusion, the local endogenous THs may be impaired during VC. T3 attenuated calcification, prevented the loss of lineage markers, restored the expression of klotho, and downregulated Runx2, Osterix, and OPN expression in rat aortas with VC. T3 may have a powerful protective effect on VC and have potential in preventing and treating VC-accompanied osteoporosis.

Acknowledgments This work was supported by the National Natural Sciences Foundation of China (Grant no. 81370972 to BH. Zhang and 30600232 to J. Zhang).

Conflict of Interest Jing Zhang, Jin-Rui Chang, Xiao-Hui Duan, Yan-Rong Yu, and Bao-Hong Zhang of the paper have no financial and personal relationships with other people or organizations that could inappropriately influence this work.

Human and Animal Rights and Informed Consent All animal care and experimental protocols complied with the Animal Management Rule of the Ministry of Health, People's Republic of China (Document No. 55, 2001).

References

1. Flamant F, Baxter JD, Forrest D, Refetoff S, Samuels H, Scanlan TS, Vennström B, Samarut J (2006) International Union of Pharmacology. LIX. The pharmacology and classification of the nuclear receptor superfamily: thyroid hormone receptors. Pharmacol Rev 58:705–711
2. Bassett JH, Williams GR (2008) Critical role of the hypothalamic-pituitary-thyroid axis in bone. Bone 43:418–426
3. Williams GR (2009) Actions of thyroid hormones in bone. Endokrynol Pol. 60:380–388
4. O'Shea PJ, Harvey CB, Suzuki H, Kaneshige M, Kaneshige K, Cheng SY, Williams GR (2003) A thyrotoxic skeletal phenotype of advanced bone formation in mice with resistance to thyroid hormone. Mol Endocrinol 17:1410–1424
5. Murphy E, Williams GR (2004) The thyroid and the skeleton. Clin Endocrinol (Oxf) 61:285–298
6. Gogakos AI, Duncan Bassett JH, Williams GR (2010) Thyroid and bone. Arch Biochem Biophys 503:129–136
7. Danzi S, Klein I (2012) Thyroid hormone and the cardiovascular system. Med Clin North Am 96:257–268
8. Biondi B, Palmieri EA, Lombardi G, Fazio S (2002) Effects of thyroid hormone on cardiac function: the relative importance of heart rate, loading conditions, and myocardial contractility in the regulation of cardiac performance in human hyperthyroidism. J Clin Endocrinol Metab 87:968–974
9. Kahaly GJ, Dillmann WH (2005) Thyroid hormone action in the heart. Endocr Rev 26:704–728
10. Klein I, Danzi S (2007) Thyroid disease and the heart. Circulation 116:1725–1735
11. Mizuma H, Murakami M, Mori M (2001) Thyroid hormone activation in human vascular smooth muscle cells: expression of type II iodothyronine deiodinase. Circ Res 88:313–318
12. Tatar E, Kircelli F, Asci G, Carrero JJ, Gungor O, Demirci MS, Ozbek SS, Ceylan N, Ozkahya M, Toz H, Ok E (2011) Associations of triiodothyronine levels with carotid atherosclerosis and arterial stiffness in hemodialysis patients. Clin J Am Soc Nephrol 6:2240–2246
13. Shaw LJ, Raggi P, Berman DS, Callister TQ (2006) Coronary artery calcium as a measure of biologic age. Atherosclerosis 188:112–119
14. Goettsch C, Hutcheson JD (2013) Aikawa EMicroRNA in cardiovascular calcification: focus on targets and extracellular vesicle delivery mechanisms. Circ Res 112(7):1073–1084
15. Shao JS, Cai J, Towler DA (2006) Molecular mechanisms of vascular calcification: lessons learned from the aorta. Arterioscler Thromb Vasc Biol 26:1423–1430
16. Demer LL, Tintut Y (2008) Vascular calcification: pathobiology of a multifaceted disease. Circulation 117:2938–2948
17. Zhu D, Mackenzie NC, Millán JL, Farquharson C, MacRae VE (2011) The appearance and modulation of osteocyte marker expression during calcification of vascular smooth muscle cells. PLoS One 6:e19595
18. Tyson KL, Reynolds JL, McNair R, Zhang Q, Weissberg PL, Shanahan CM (2003) Osteo/chondrocytic transcription factors and their target genes exhibit distinct patterns of expression in human arterial calcification. Arterioscler Thromb Vasc Biol 23:489–494
19. Li X, Yang HY, Giachelli CM (2008) BMP-2 promotes phosphate uptake, phenotypic modulation, and calcification of human vascular smooth muscle cells. Atherosclerosis. 199:271–277
20. Nakahara T, Sato H, Shimizu T, Tanaka T, Matsui H, Kawai-Kowase K, Sato M, Iso T, Arai M, Kurabayashi M (2010) Fibroblast growth factor-2 induces osteogenic differentiation through a Runx2 activation in vascular smooth muscle cells. Biochem Biophys Res Commun. 394:243–248
21. Nakashima K, Zhou X, Kunkel G, Zhang Z, Deng JM, Behringer RR, de Crombrugghe B (2002) The novel zinc finger-containing transcription factor osterix is required for osteoblast differentiation and bone formation. Cell 108:17–29
22. Pan K, Sun Q, Zhang J, Ge S, Li S, Zhao Y, Yang P (2010) Multilineage differentiation of dental follicle cells and the roles of Runx2 over-expression in enhancing osteoblast/cementoblast-related gene expression in dental follicle cells. Cell Prolif 43:219–228
23. Lim K, Lu TS, Molostvov G, Lee C, Lam FT, Zehnder D, Hsiao LL (2012) Vascular Klotho deficiency potentiates the development of human artery calcification and mediates resistance to fibroblast growth factor 23. Circulation 125:2243–2255
24. Niederhoffer N, Bobryshev YV, Lartaud-Idjouadiene I, Giummelly P, Atkinson J (1997) Aortic calcification produced by vitamin D3 plus nicotine. J Vasc Res 34:386–398
25. Hyder JA, Allison MA, Criqui MH, Wright CM (2007) Association between systemic calcified atherosclerosis and bone density. Calcif Tissue Int 80:301–306
26. Toussaint ND, Lau KK, Strauss BJ, Polkinghorne KR, Kerr PG (2008) Associations between vascular calcification, arterial stiffness and bone mineral density in chronic kidney disease. Nephrol Dial Transplant 23:586–593
27. Raggi P, Bellasi A, Ferramosca E, Block GA, Muntner P (2007) Pulse wave velocity is inversely related to vertebral bone density in hemodialysis patients. Hypertension 49:1278–1284
28. Persy V, D'Haese P (2009) Vascular calcification and bone disease: the calcification paradox. Trends Mol Med 15(9):405–416
29. Kim ES, Shin JA, Shin JY, Lim DJ, Moon SD, Son HY, Han JH (2012) Association between low serum free thyroxine concentrations and coronary artery calcification in healthy euthyroid subjects. Thyroid 22(9):870–876
30. Takamura N, Akilzhanova A, Hayashida N, Kadota K, Yamasaki H, Usa T, Nakazato M, Maeda T, Ozono Y, Aoyagi K (2009) Thyroid function is associated with carotid intima-media thickness in euthyroid subjects. Atherosclerosis 204(2):e77–e81

31. Sato Y, Nakamura R, Satoh M, Fujishita K, Mori S, Ishida S, Yamaguchi T, Inoue K, Nagao T, Ohno Y (2005) Thyroid hormone targets matrix Gla protein gene associated with vascular smooth muscle calcification. Circ Res 97:550–557
32. Aoshima Y, Mizobuchi M, Ogata H, Kumata C, Nakazawa A, Kondo F, Ono N, Koiwa F, Kinugasa E, Akizawa Vitamin T (2012) D receptor activators inhibit vascular smooth muscle cell mineralization induced by phosphate and TNF-α. Nephrol Dial Transplant 27:1800–1806
33. Ciceri P, Volpi E, Brenna I, Arnaboldi L, Neri L, Brancaccio D, Cozzolino M (2012) Combined effects of ascorbic acid and phosphate on rat VSMC osteoblastic differentiation. Nephrol Dial Transplant 27:122–127
34. Byon CH, Sun Y, Chen J, Yuan K, Mao X, Heath JM, Anderson PG, Tintut Y, Demer LL, Wang D, Chen Y (2011) Runx2-upregulated receptor activator of nuclear factor κB ligand in calcifying smooth muscle cells promotes migration and osteoclastic differentiation of macrophages. Arterioscler Thromb Vasc Biol 31:1387–1396
35. Tanaka T, Sato H, Doi H, Yoshida CA, Shimizu T, Matsui H, Yamazaki M, Akiyama H, Kawai-Kowase K, Iso T, Komori T, Arai M, Kurabayashi M (2008) Runx2 represses myocardin-mediated differentiation and facilitates osteogenic conversion of vascular smooth muscle cells. Mol Cell Biol 28:1147–1160
36. Nishio Y, Dong Y, Paris M, O'Keefe RJ, Schwarz EM, Drissi H (2006) Runx2-mediated regulation of the zinc finger Osterix/Sp7 gene. Gene 372:62–70
37. Lee CH, Huang YL, Liao JF, Chiou WF (2011) Ugonin K promotes osteoblastic differentiation and mineralization by activation of p38 MAPK- and ERK-mediated expression of Runx2 and osterix. Eur J Pharmacol 668:383–389